Near-infrared fluorescence imaging in colorectal cancer and its metastases

Meijer, R.P.J.

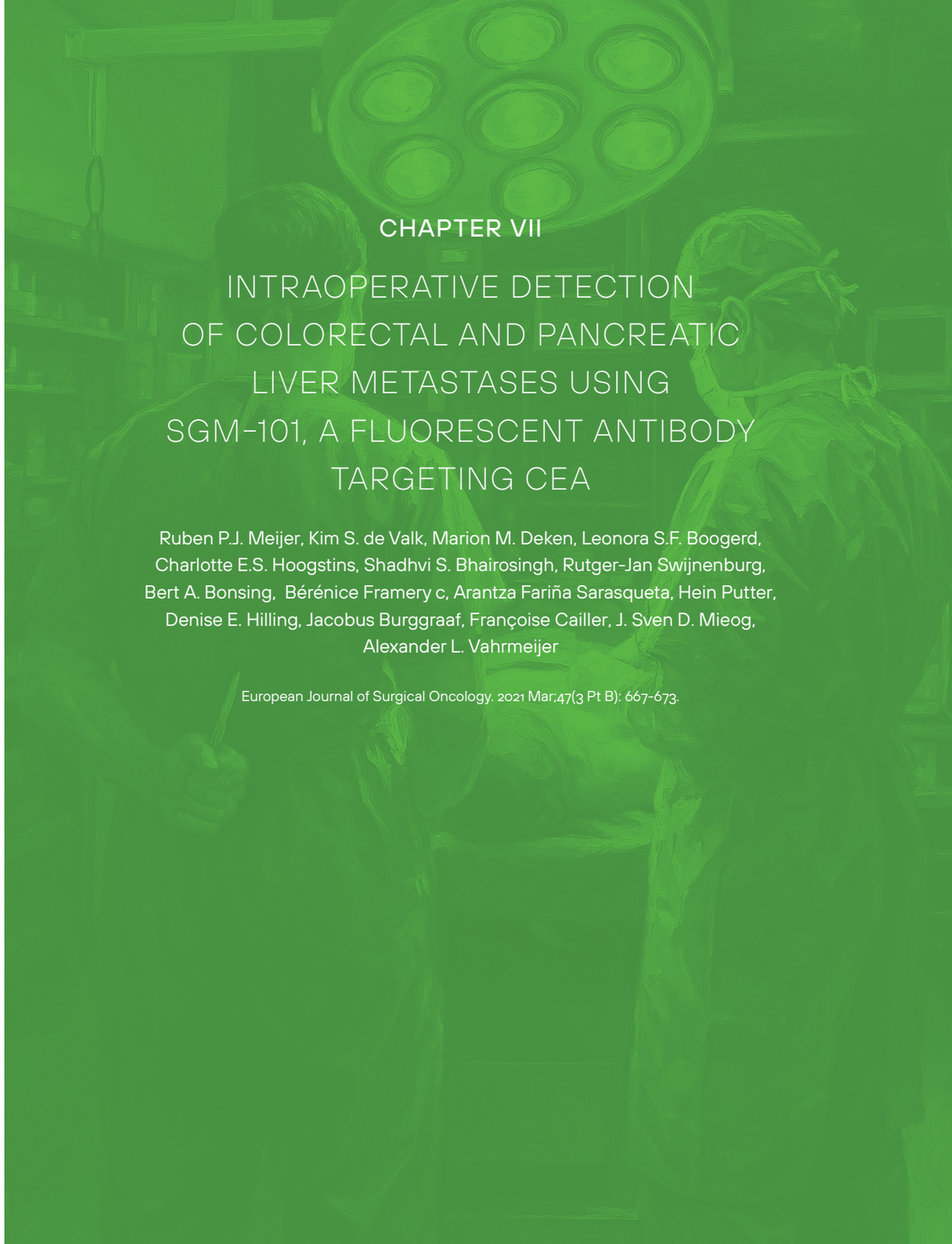

CHAPTER VII

INTRAOPERATIVE DETECTION OF COLORECTAL AND PANCREATIC LIVER METASTASES USING SGM-101, A FLUORESCENT ANTIBODY TARGETING CEA

Ruben P.J. Meijer, Kim S. de Valk, Marion M. Deken, Leonora S.F. Boogerd, Charlotte E.S. Hoogstins, Shadhvi S. Bhairosingh, Rutger-Jan Swijnenburg, Bert A. Bonsing, Bérénice Framery c, Arantza Fariña Sarasqueta, Hein Putter, Denise E. Hilling, Jacobus Burggraaf, Françoise Cailler, J. Sven D. Mieog, Alexander L. Vahrmeijer

European Journal of Surgical Oncology. 2021 Mar;47(3 Pt B): 667-673.

Abstract

BACKGROUND Fluorescence-guided surgery can provide surgeons with an imaging tool for real-time intraoperative tumor detection. SGM-101, an anti-CEA antibody labelled with a fluorescent dye, is a tumor-specific imaging agent that can aid in improving detection and complete resection for CEA-positive tumors. In this study, the performance of SGM-101 for the detection of colorectal and pancreatic liver metastases was investigated.

METHODS In this open-label, non-randomized, single-arm pilot study, patients were included with liver metastases from colorectal origin and intraoperatively detected liver metastases from pancreatic origin (during planned pancreatic surgery). SGM-101 was administered two to four days before the scheduled surgery as a single intravenous injection. Intraoperative fluorescence imaging was performed using the Quest Spectrum® imaging system. The performance of SGM-101 was assessed by measuring the intra-operative fluorescence signal and comparing this to histopathology.

RESULTS A total of 19 lesions were found in 11 patients, which were all suspected as malignant in white light and subsequent fluorescence inspection. Seventeen lesions were malignant with a mean tumor-to-background ratio of 1.7. The remaining two lesions were false-positives as proven by histology.

CONCLUSION CEA-targeted fluorescence-guided intraoperative tumor detection with SGM-101 is feasible for the detection of colorectal and pancreatic liver metastases.

Introduction

Tumor-targeted near-infrared (NIR) fluorescence imaging is a surgical technique that allows real-time detection of malignant tissue to aid surgeons in the peroperative decision making.[1] The added value of tumor-targeted fluorescence imaging is twofold: identification of novel, mostly small malignant lesions and prevention of tumor-positive resection margins.[2,3]

Achieving a complete resection is of utmost importance during oncologic surgery. Especially for colorectal liver metastases, in which a tumor-positive resection margin (<1 mm) is one of the main factors associated with limited overall survival.[4] Unfortunately, margin-positive resections are found in 12%-28% of the patients after liver metastasectomy.[5-7] In pancreatic cancer, intraoperative detection of occult liver metastases immediately translates into a change in treatment strategy, mostly palliation.[8,9] Therefore, adequate pre- and intraoperative staging is important in this vulnerable patient population to avoid a futile high-risk resection.

Preoperative imaging modalities, such as computed tomography (CT), positron emission tomography (PET), and magnetic resonance imaging (MRI), used for the detection of possible liver metastases lack sensitivity for subcentimeter and (sub)capsular lesions.[10-12] Intraoperative detection, by means of palpation, visual inspection, and ultrasonography (in case of deep-seated tumors) is therefore of great importance. With this in mind, real-time intraoperative fluorescence imaging can be a useful tool for surgeons, as it is known to have a high sensitivity in identifying small, superficially located malignant lesions in the liver.[13-15] Additionally, due to the growing use of minimally-invasive procedures, fluorescence imaging can be beneficial as it enhances the visual inspection, thereby compensating for the lack of tactile feedback.

The carcinoembryonic antigen (CEA) is overexpressed in more than 90% of colorectal and 70% of pancreatic adenocarcinomas.[16,17] SGM-101 (SurgiMab, Montpellier, France) is a chimeric antibody targeting CEA, labelled with a fluorescent dye, making it a promising tumor-targeted agent for imaging of CEA-positive cancers. Recent publications have shown promising results in the field of fluorescence-guided surgery using SGM-101.[3,18,19] In complex colorectal cancer, fluorescence imaging with SGM-101 resulted in the additional identification of malignant lesions in 43% of the patients.[3] These lesions were not detected by preoperative imaging or with the naked eye during surgery and were only detected with fluorescence imaging, resulting in a change in treatment strategy

in 35% of the patients.[3] Moreover, the intravenous injection of SGM-101 was considered safe as no related (serious) adverse events were reported in these patients.[3] SGM-101 was further evaluated in additional patients with pancreatic ductal adenocarcinoma and primary and recurrent colorectal cancer to assess the safety, efficacy and optimal dose of SGM-101. The aim of this study was to assess the performance of SGM-101 for the detection of colorectal and pancreatic liver metastases.

Methods

The study was an open-label, non-randomized, single-arm pilot study performed in eleven patients with colorectal or pancreatic adenocarcinoma metastasized to the liver, to evaluate the performance of SGM-101 for the detection of these liver metastases. In the pancreatic cancer patients, the liver metastases were found during the explorative phase of the surgical procedure and were not diagnosed upfront by routine imaging techniques.

Four of these 11 patients have previously been described.[3,18] The study was a collaborative effort between SurgiMab (Sponsor; Montpellier, France), the Centre for Human Drug Research (CHDR; Leiden, the Netherlands) and the Department of Surgery of Leiden University Medical Center (LUMC; Leiden, the Netherlands). The study was approved by a certified medical ethics review board (Stichting BEBO, Assen, the Netherlands) and performed in accordance with the laws and regulations on drug research in humans of the Netherlands. The study is registered in ClinicalTrials.gov under identifier NCT02973672 and aimed to include patients with primary and recurrent colorectal cancer and primary pancreatic cancer. For the current analysis only patients with liver metastases were subtracted from the total group to determine the potential of CEA-targeted fluorescence imaging for liver metastases.

Patients were included in the study after evaluation in a multidisciplinary team meeting and met the following inclusion criteria: aged over 18 years with elevated serum CEA levels (>3 ng/ ml) and scheduled for a surgical resection of colorectal liver metastases or exploration of pancreatic ductal adenocarcinoma with possible subsequent resection of the primary tumor. The exclusion criteria ruled out pregnancy, history of (severe) allergic reactions, impaired renal or hepatic function, and a diagnosis of another malignancy in the last 5 years. All subjects provided written informed consent to the investigators prior to the start of any study-related procedure.

SGM-101 is a CEA-specific chimeric antibody conjugated to a NIR emitting fluorochrome with a fluorescence peak around 705 nm.[20] Intravenous administration of SGM-101 (5-15 mg over 30 min) was performed at the CHDR, where patients were admitted 2e4 days before their scheduled surgery. After infusion, patients were observed for at least 6 hours for safety and tolerability assessments. Plasma CEA levels were determined before and after administration of SGM-101.

All patients underwent the scheduled surgical procedure at LUMC according to standard of care by certified HPB surgeons who were familiar with fluorescence imaging. First, the surgical field was explored under white light using standard visual and tactile methods and subsequently completed with ultrasound imaging based on the surgeon's preference. Next, fluorescence imaging was performed, using the Quest Spectrum® (Quest Medical Imaging BV, Middenmeer, The Netherlands). This imaging system can measure at two different wavelengths. For this study, the tissue was illuminated with 680 nm laser light and visualized at approximately 710 nm.

Every liver lesion was recorded as 1) suspect or not suspect for malignancy as assessed on preoperative imaging 2) suspect or not suspect for malignancy as assessed with the naked eye under white light during surgery and 3) suspect or not suspect for malignancy as assessed with fluorescence imaging. It was the surgeon's decision whether resection of the suspected liver lesion was feasible (which applied to both fluorescent and non-fluorescent lesions) and if intraoperative frozen sections (e.g. in case of pancreatic cancer) were needed for histologic confirmation.

Images obtained with the Quest Spectrum® were viewed and processed with the use of the Architector Vision Suite (version 1.8.3; Quest Medical Imaging, Middenmeer, the Netherlands). For every fluorescent lesion, an intraoperative tumor-to-background ratio (TBR) was calculated, using ImageJ (version 1.51j8; National Institute of Health, MD, USA). The TBR was calculated by dividing the quotient of the signal intensity of a region of interest (ROI) selected in the tumorous tissue with an ROI located in the directly surrounding liver parenchyma.

Due to the exploratory nature of the study, the sample size was not based on statistical considerations. For statistical analysis, IBM SPSS Statistics (Version 25, La Jolla, CA, USA) was used. To explore a possible TBR difference between the different dosing groups a Kruskal-Wallis test was conducted. $P < 0.05$ was considered as significant.

All resected lesions were assessed at the Department of Pathology using a standardized pathology manual designed for fluorescence-guided surgery

studies, including immunohistochemistry analysis with haematoxylin and eosin (H&E) staining and CEA staining on 4 mm formalin-fixed, paraffin-embedded sections. These tissue sections were scored for expression of CEA using the total immunostaining score (TIS), by multiplying the percentage score (PS) and intensity score (IS) found. The PS represented the percentage of positively stained cells and ranged between 0 and 4 (0: none, 1: <10%, 2: 10-50%, 3: 51-80%, 4: >80%). The IS represented the intensity of the stained cells and ranged between 0 and 3.

(0: no staining, 1: mild, 2: moderate, 3: intense). The calculated TIS was then defined as negative (0), weak (1-4), moderate (6-8) or intense (9-12).

For all lesions, the definitive histological diagnosis was compared with the clinical white light assessment and the fluorescence imaging data to determine concordance. A confirmed malignant lesion which was fluorescent during surgery was considered a true-positive. A malignant lesion without fluorescence during surgery was a false-negative. Benign lesions without fluorescence during surgery were considered as true-negative and finally, benign lesions that emitted fluorescence during surgery were considered as false-positive.

Results

From January 2016 to January 2019, a total of 11 patients (9 males and 2 females; median age 70 years) were included in this study (Table 1). Eight patients had highly suspect liver metastases from colorectal origin and three patients were scheduled for an exploration and potential resection for pancreatic ductal adenocarcinoma. All patients received SGM-101 and underwent the scheduled surgery (10 open procedures, 1 laparoscopic procedure). Patients were scheduled for a liver metastasectomy for colorectal metastases (n = 6), exploration and potential pancreatoduodenectomy (n = 3), sigmoid resection with synchronous liver metastasectomy (n = 1) and low anterior resection with synchronous liver metastasectomy (n = 1; Table 1). All serum CEA-levels decreased after injection with SGM-101. No adverse events (AEs) or serious adverse events (SAEs) were reported that were directly related to SGM-101.

TABLE 1 Patient characteristics.

Demographics				SGM-101 dosing			Diagnosis		
ID	Age	Sex	CEA serum level pre-injection (µg/L)	Dose (mg)	Interval (days)	CEA serum level post-injection (µg/L)	Primary carcinoma	In situ	Executed procedure
1	71	M	10.6	5	2	1.1	Pancreas	Yes	Aborted PS (o)
2	68	M	23.5	7.5	2	1.0	Pancreas	Yes	Aborted PS (l)
3	71	M	41.1	7.5	4	13.9	Pancreas	Yes	Aborted PS (o)
4	64	M	9.1	7.5	4	1.5	Sigmoid	Yes	Sigmoid resection with LM (o)
5	72	M	49.9	10	4	U	Sigmoid	No	LM (o)
6	70	F	5.3	10	4	2.5	Sigmoid	No	LM (o)
7	76	M	5.0	10	4	0.4	Colon	No	LM (o)
8	61	F	46.2	10	4	44.2	Sigmoid	No	Aborted LM (o)
9	59	M	147.8	10	4	30.9	Rectal	Yes	LM (o)
10	44	M	140.7	12.5	4	U	Sigmoid	Yes	Low anterior resection with LM (o)
11	73	M	11.5	15	4	U	Rectal	No	LM (o)

Abbreviations: CEA carcinoembryonic antigen, M Male, PS pancreatic surgery, O open, LM liver metastasectomy, F Female, L laparoscopic, U unknown.

TABLE 2 Intraoperative and pathology results.

		Intraoperative					Pathology				IHC		
ID	Lesion	Location (segment)	WLS	IOUS	NIR	TBR	Histopathology	Size (MM)	Tumor free margin (MM)	Concor-dance	IS	PS	TIS
1	1	2	+	NA	+	1.37	Adenocarcinoma	NA	NA	TP	3	4	12
2	2	2	+	NA	+	1.41	Adenocarcinoma	NA	NA	TP	1	1	1
	3	3	+	NA	+	1.19	Adenocarcinoma	NA	NA	TP	3	4	12
3	4	4	+	NA	+	2.39	Adenocarcinoma	NA	NA	TP	3	4	12
	5	4	+	NA	+	2.00	Adenocarcinoma	NA	NA	TP	3	4	12
4	6	2/3	+	+	+	1.55	Adenocarcinoma	17	4	TP	3	4	12
	7	4B	+	+	+	1.72	Adenocarcinoma	13	15	TP	3	4	12
	8	6	+	+	+	1.43	Adenocarcinoma	11	5	TP	3	4	12
5	9	8	+	+	+	1.55	Calcified nodule	NA	NA	FP	0	1	0
	10	6	+	+	+	1.99	Adenocarcinoma	22	7	TP	3	4	12
	11	6/7	+	+	+	1.46	Adenocarcinoma	14	12	TP	3	4	12
6	12	6	+	+	+	2.03	Adenocarcinoma	38	R1	TP	3	4	12
7	13	7/8	+	+	+	2.10	Adenocarcinoma	28	6	TP	3	4	12
8	14	6	+	+	+	1.31	Adenocarcinoma	NA	NA	TP	3	4	12
9	15	8	+	+	+	1.80	Adenocarcinoma	85	3	TP	3	4	12
	16	8/9	+	+	+	2.04	Adenocarcinoma	32	3	TP	3	4	12
10	17	8	+	+	+	1.32	Adenocarcinoma	7	1	TP	3	4	12
11	18	6	+	+	+	1.31	Liver parenchyma	NA	NA	FP	0	1	0
	19	2/3	+	+	+	1.15	Adenocarcinoma	16	80	TP	3	4	12

Abbreviations: IHC immunohistochemistry, WLS White Light Suspect, IOUS intraoperative ultrasound, NIR Near Infrared Suspect, TBR Tumor-to-background ratio, MM milli- meter, IS *Intensity Score,* PS Percentage Score, TIS Total Immunostaining Score, U unknown, + Positive, NA not applicable, TP true-positive, FP false-positive.

LESIONS

A total of 19 lesions were resected (Table 2). All lesions were suspected for malignancy under white light and with intraoperative ultrasound, as well as with fluorescence imaging (figure 1 and figure 2). Seventeen lesions were confirmed malignant by histological evaluation. These 17 lesions had a mean TBR of 1.7 (range 1.2-2.4) with the highest median TBR of 2.0 found in the group dosed with 10 mg 4 days before surgery (figure 3, p = 0.235). The two false-positive lesions were a calcified nodule with inflammation and steatosis (lesion 5, TBR 1.6) and normal liver parenchyma (Lesion 11, TBR 1.3).

Radicality assessment was possible in 11 lesions, as lesion 1-5 and 14 were intraoperative frozen sections of which radicality could not be evaluated with certainty. Of the evaluated lesions, one lesion was irradically resected with microscopic tumor invasion of the resection margin (Lesion 12). The planned surgical procedure (Whipple or pancreatic tail resection) was aborted in all patients with pancreatic ductal adenocarcinoma immediately after histological confirmation with intraoperative frozen section analysis of the liver metastases. In one patient with colorectal liver metastases (patient ID 8), multiple small lesions in different segments of the liver were detected (both in white light and with fluorescence) and were confirmed malignant at frozen section analysis leading to a non-curative situation as decided by the surgeon.

FIGURE 1 Fluorescence evaluation of a colorectal liver metastasis (Patient 4, Lesion 8).
A. Intraoperative fluorescence imaging shows clear fluorescence at the tumor site (liver segment 6, TBR 1.4). Note the intense auto-fluorescence signal from the surgical gloves. **B.** *Ex vivo* breadloafs from the lesion in A show co-localisation of fluorescence with visual tumor localisation. **C.** Staining with hematoxylin and eosin (H&E) and for carcinoembryonic antigen (CEA). Total immunostaining score (TIS) of 12, the CEA pattern corresponds to the site containing tumor cells visible on H&E staining.

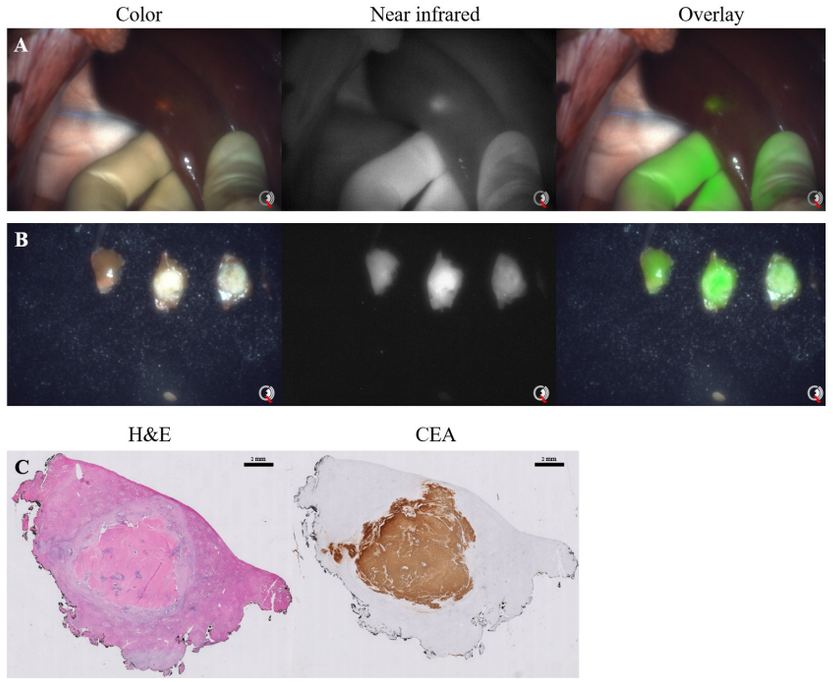

FIGURE 2 Fluorescence evaluation of a liver metastasis from a pancreatic ductal adenocarcinoma (Patient 3, Lesion 4).
A. Intraoperative fluorescence imaging showed clear fluorescence at the tumor site (liver segment 4, TBR 2.4). **B.** *Ex vivo* back table image from the lesion in A shows co-localisation of fluorescence with visual tumor localisation. **C.** Staining with hematoxylin and eosin (H&E) and for carcinoembryonic antigen (CEA). Total immunostaining score (TIS) of 12, the CEA pattern corresponds to the site containing tumor cells visible on H&E staining.

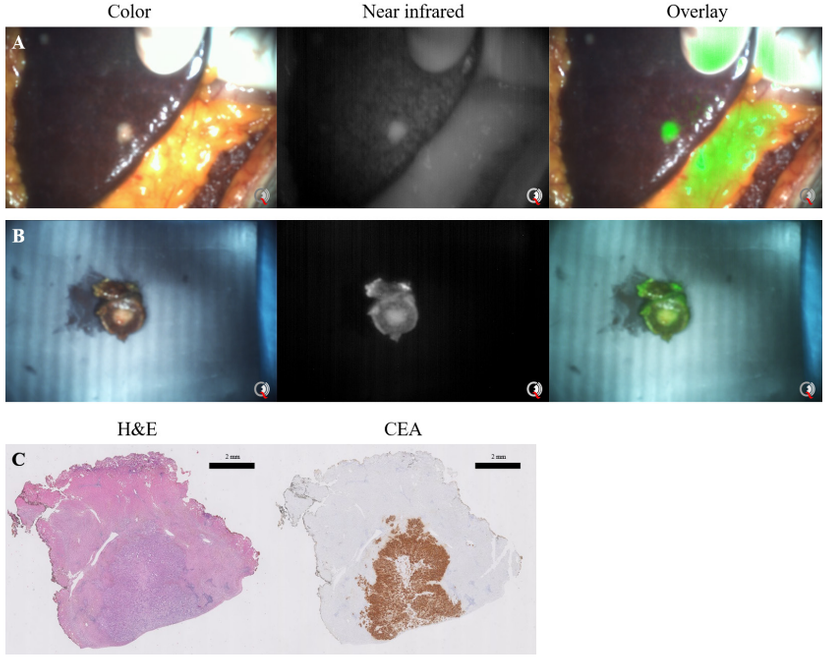

FIGURE 3 Scatter plot of the tumor-to-background ratios of all malignant lesions.
Every true-positive lesion is presented as an individual point. The median per dose is presented with a horizontal line (p ¼ 0.235).

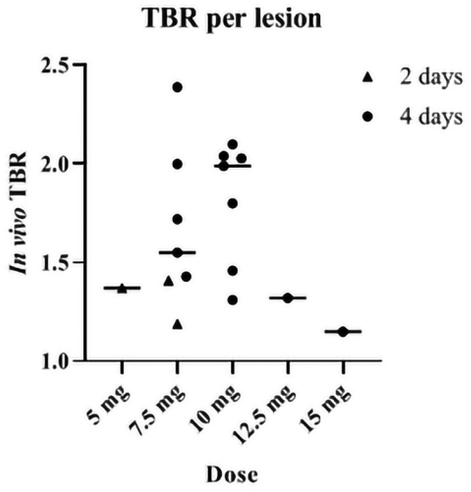

IMMUNOHISTOCHEMISTRY

Sixteen out of 17 true-positive lesions had a maximum TIS of 12 (Table 2). One true-positive lesion was weak for CEA expression (TIS 1, TBR 1.4). Both false-positive liver lesions were negative for CEA-expression (TIS 0, TBR 1.5 and 1.3).

Discussion

This study describes the first series of intraoperative fluorescence imaging for the detection of liver metastases using a tumor-targeted agent. SGM-101 enabled detection of all liver metastases of pancreatic and colorectal origin and resulted in an 89% accuracy rate without any false-negative lesions.

A limitation of this study is the small sample size of 11 patients. This is a consequence of the decision to analyse 2 subgroups (liver metastases and peritoneal metastases) separate from the main study population (primary and recurrent colorectal cancer and primary pancreatic cancer).[3,18,19] Moreover, we decided to combine the results from colorectal and pancreatic liver metastases, as both entities are CEA-positive in most cases, to show the potential of CEA-targeted fluorescence imaging in these patients.

The current marketing information on SGM-101 is insufficient to elaborate on the cost of the procedure and the possible subsequent financial benefit. The costs for fluorescence-guided surgery in general are incurred through the one-time purchase of an imaging system and the use a fluorescent agent. These costs will, most likely, be compensated by a reduction in complications and improved patient outcomes.

The majority of the resected liver metastases in this study were true-positives (17 out of 19). Only two lesions were reported as false-positives but were also suspected as malignant under white light. However, both these false-positive lesions did not show any CEA expression with immunohistochemistry, making it plausible that fluorescence was triggered by other factors, such as auto-fluorescence which is known to be more common for this wavelength (700 nm).[21] Another explanation may be the enhanced permeability retention effect, in which macromolecular drugs (such as antibodies) tend to accumulate in tissue with hypervascularisation and compromised lymphatic drainage.[22]

During fluorescence imaging intraoperative TBR measurements should be considered leading, as tissue resection and decision making occurs during surgery, while the tissue is still inside the patient. However, current commercially available imaging systems cannot calculate the TBR in real-time. Therefore, TBRs are calculated after the procedure. In this study, a mean intraoperative TBR of 1.7 was found, which is relatively high given the fact that SGM-101 is cleared by the liver. This is most likely a consequence of the relatively long interval from injection till surgery, as the mainstream of patients were administered with SGM-101 4 days before surgery, which potentially lowers the background in the liver and thus increases the TBR. Previously, Cetuximab-IRDye800, a NIR fluorescent agent, targeting the epidermal growth factor receptor (EGFR), was used for the intraoperative detection of pancreatic cancer.[23] Interestingly, liver metastases were detected by negative contrast. This might be a consequence of the relative high dye/protein ratio (1.8) of Cetuximab-IRDye800 and a higher EGFR expression in healthy hepatocytes compared to the tumor cells. The dye/protein ratio for SGM-101 is 1.6, which is approximately the same as for Cetuximab-IRDye800. Nevertheless, CEA-expression in the tumor surrounding hepatocytes was not detected, explaining the clear contrast found in our cohort.

Immediate back table imaging of resected liver lesions can be used to identify positive resection margins. Additionally, these images can be compared to the intraoperative images of the wound bed to recognize any remaining fluorescence and thus a potential margin-positive resection, which can be addressed immediately. Given the margin-positive resection rate of up to 28% in liver metastasectomy patients, identification of remaining malignancy at the wound bed can lead to a direct re-resection and change an R1 resection into a R0 resection.[5] In this patient series, in 1 out of 11 assessable lesions, the resection margin was positive for tumor. Unfortunately, assessment of fluorescence at the wound bed was not recorded in this study.

In 2009, Ishizawa *et al.*, described the results of indocyanine green (ICG) for the detection of liver metastases and primary liver malignancies.[24] ICG causes a fluorescent rim, due to the accumulation of ICG in the tumor surrounding hepatocytes. Our group previously reported the identification of additional liver lesions using ICG in approximately 12% of patients.[13-15] The current study with SGM-101 did not show detection of additional liver lesions, which might be a consequence of the small study population and the inclusion of four patients with irresectable disease (patient ID 1-3 and 8). However, SGM-101 is, opposed to ICG, tumor-specific. As a CEA-targeting antibody, SGM-101 has the possibility to detect other types of metastases (eg. peritoneal), as well as the primary tumor. Therefore, SGM-101 seems to be a promising alternative or adjunct to ICG, especially in those patients who still have their primary tumor in situ or have a high probability of synchronous metastases (i.e. liver or peritoneal metastases). A larger study is currently being prepared and expected to start in the first quarter of 2021, to assess the added value of SGM-101 for the detection of additional liver metastases and tumor-positive resection margins, potentially in combination with ICG. A benefit of the combination SGM-101 and ICG, is that these agents work on different wavelengths (700 nm and 800 nm, respectively) and provide tumor detection with a different mechanism. With the use of a NIR camera system that has the ability to image both wavelengths independently, one can switch between those wavelengths without interference.

Conclusion

All liver metastases from colorectal and pancreatic origin were fluorescent with SGM-101, administered 2-4 days prior to surgery. These results warrant further research to determine the added value of this technique.

REFERENCES

1 Vahrmeijer AL, Hutteman M, van der Vorst JR, van de Velde CJ, Frangioni JV. Image-guided cancer surgery using near-infrared fluorescence. Nat Rev Clin Oncol 2013;10(9):507e18.

2 Harlaar NJ, Koller M, de Jongh SJ, van Leeuwen BL, Hemmer PH, Kruijff S, *et al.* Molecular fluorescence-guided surgery of peritoneal carcinomatosis of colorectal origin: a single-centre feasibility study. Lancet Gastroenterol Hepatol 2016;1(4):283e90.

3 Boogerd LSF, Hoogstins CES, Schaap DP, Kusters M, Handgraaf HJM, van der Valk MJM, *et al.* Safety and effectiveness of SGM-101, a fluorescent antibody targeting carcinoembryonic antigen, for intraoperative detection of colorectal cancer: a dose-escalation pilot study. Lancet Gastroenterol Hepatol 2018;3(3): 181e91.

4 Margonis GA, Sergentanis TN, Ntanasis-Stathopoulos I, Andreatos N, Tzanninis IG, Sasaki K, *et al.* Impact of surgical margin width on recurrence and overall survival following Ro hepatic resection of colorectal metastases: a systematic review and meta-analysis. Ann Surg 2018;267(6):1047e55.

5 Fretland AA, Dagenborg VJ, Bjornelv GMW, Kazaryan AM, Kristiansen R, Fagerland MW, *et al.* Laparoscopic versus open resection for colorectal liver metastases: the OSLO-COMET randomized controlled trial. Ann Surg 2018;267(2):199e207.

6 Postriganova N, Kazaryan AM, Rosok BI, Fretland A, Barkhatov L, Edwin B. Margin status after laparoscopic resection of colorectal liver metastases: does a narrow resection margin have an influence on survival and local recurrence? HPB 2014;16(9):822e9.

7 Montalti R, Tomassini F, Laurent S, Smeets P, De Man M, Geboes K, *et al.* Impact of surgical margins on overall and recurrence-free survival in parenchymal-sparing laparoscopic liver resections of colorectal metastases. Surg Endosc 2015;29(9):2736e47.

8 Seufferlein T, Porzner M, Becker T, Budach V, Ceyhan G, Esposito I, *et al.* [S3-guideline exocrine pancreatic cancer]. Z Gastroenterol 2013;51(12): 1395e440.

9 Tempero MA, Malafa MP, Behrman SW, Benson 3rd AB, Casper ES, Chiorean EG, *et al.* Pancreatic adenocarcinoma, version 2.2014: featured up-dates to the NCCN guidelines. J Natl Compr Canc Netw 2014;12(8):1083e93.

10 Niekel MC, Bipat S, Stoker J. Diagnostic imaging of colorectal liver metastases with CT, MR imaging, FDG PET, and/or FDG PET/CT: a meta-analysis of prospective studies including patients who have not previously undergone treatment. Radiology 2010;257(3):674e84.

11 Kaibori M, Matsui K, Ishizaki M, Iida H, Okumura T, Sakaguchi T, *et al.* Intra-operative detection of superficial liver tumors by fluorescence imaging using indocyanine green and 5-aminolevulinic acid. Anticancer Res 2016;36(4): 1841e9.

12 Peloso A, Franchi E, Canepa MC, Barbieri L, Briani L, Ferrario J, *et al.* Combined use of intraoperative ultrasound and indocyanine green fluorescence imaging to detect liver metastases from colorectal cancer. HPB 2013;15(12):928e34.

13 Handgraaf HJM, Boogerd LSF, Hoppener DJ, Peloso A, Sibinga Mulder BG, Hoogstins CES, *et al.* Long-term follow-up after near-infrared fluorescence-guided resection of colorectal liver metastases: a retrospective multicenter analysis. Eur J Surg Oncol 2017;43(8):1463e71.

14 Boogerd LS, Handgraaf HJ, Lam HD, Huurman VA, Farina-Sarasqueta A, Frangioni JV, *et al.* Laparoscopic detection and resection of occult liver tumors of multiple cancer types using real-time near-infrared fluorescence guidance. Surg Endosc 2017;31(2):952e61.

15 van der Vorst JR, Schaafsma BE, Hutteman M, Verbeek FP, Liefers GJ, Hartgrink HH, *et al.* Near-infrared fluorescence-guided resection of colorectal liver metastases. Cancer 2013;119(18):3411e8.

16 Tiernan JP, Perry SL, Verghese ET, West NP, Yeluri S, Jayne DG, *et al.* Carcinoembryonic antigen is the preferred biomarker for *in vivo* colorectal cancer targeting. Br J Canc 2013;108(3):662e7.

17 de Geus SW, Boogerd LS, Swijnenburg RJ, Mieog JS, Tummers WS, Prevoo HA, *et al.* Selecting tumor-specific molecular targets in pancreatic adenocarcinoma: paving the way for image-guided pancreatic surgery. Mol Imag Biol 2016;18(6):807e19.

18 Hoogstins CES, Boogerd LSF, Sibinga Mulder BG, Mieog JSD, Swijnenburg RJ, van de Velde CJH, *et al.* Image-guided surgery in patients with pancreatic cancer: first results of a clinical trial using SGM-101, a novel carcinoembryonic antigen-targeting, near-infrared fluorescent agent. Ann Surg Oncol 2018;25(11):3350e7.

19 Schaap DP, de Valk KS, Deken MM, Meijer RPJ, Burggraaf J, Vahrmeijer AL, *et al.* Carcinoembryonic antigen-specific, fluorescent image-guided cytoreductive surgery with hyperthermic intraperitoneal chemotherapy for metastatic colorectal cancer. Br J Surg 2020;107(4):334e7.

20 Gutowski M, Framery B, Boonstra MC, Garambois V, Quenet F, Dumas K, *et al.* SGM-101: an innovative near-infrared dye-antibody conjugate that targets CEA for fluorescence-guided surgery. Surg Oncol 2017;26(2):153e62.

21 DeLong JC, Hoffman RM, Bouvet M. Current status and future perspectives of fluorescence-guided surgery for cancer. Expert Rev Anticancer Ther 2016;16(1):71e81.

22 Maeda H. Tumor-selective delivery of macromolecular drugs via the EPR effect: background and future prospects. Bioconjugate Chem 2010;21(5): 797e802.

23 Tummers WS, Miller SE, Teraphongphom NT, Gomez A, Steinberg I, Huland DM, *et al.* Intraoperative Pancreatic Cancer Detection using Tumor-Specific Multimodality Molecular Imaging. Ann Surg Oncol. 2018;25(7): 1880e8.

24 Ishizawa T, Fukushima N, Shibahara J, Masuda K, Tamura S, Aoki T, *et al.* Real-time identification of liver cancers by using indocyanine green fluorescent imaging. Cancer 2009;115(11):2491e504.